IONIZATIONAL IGNITION AT THE INLET OF AN MPD THRUSTER

E. J. Sheppard* and M. Martinez-Sanchez†
Department of Aeronautics and Astronautics
Massachusetts Institute of Technology
Cambridge, MA 02139, U.S.A.‡

Abstract

This paper presents work aimed at understanding the inlet flow in an MPD thruster, where a transition between a cold gas and a plasma takes place (identified as steady flow ignition). Two isothermal models are presented. The first is a constant velocity case, which yields an ignition/extinction constraint on either the flow speed or mass flow. The second model considers a plasma accelerating due to both pressure and self-field magnetic forces.

Nomenclature

$\bar{c}$	a thermal speed.
B	magnetic field.
C_a	modified ambipolar coefficient $= D_a n_H$
D_a	ambipolar diffusion coefficient.
e	electron charge.
E	electric field.
E_{ion}	ionization potential of Argon I.
h	channel height/$\sqrt{12}$.
k_B	boltzmann constant.
l	a scale length.
L	thruster characteristic length.
$\dot{m}$	mass flow rate.
m	particle mass.
n	particle number density.
p	pressure.
q	critical value of α in conductivity equation.
R_m	magnetic Reynolds number, $R_m = \mu\sigma u L$.
S_{ion}	ionization rate coefficient.
T	particle temperature.
u	plasma bulk velocity.
V	slip speed.
w	channel width.
x	streamwise coordinate.
α	ionization fraction, $\alpha = \frac{n_e}{n_H}$.
Γ	ion slip flux.
θ	the temperature ratio: $\frac{T_H}{T_e + T_H}$.
Θ_{ion}	collisional rate parameter, $\frac{k_B T_e}{E_{ion}}$.
Λ_m	magnetic interaction length.
σ	scalar conductivity.
	Subscripts:
a	ambipolar diffusion
d	diffusion
e	electrons
H	heavy species = neutrals + ions
i	ions
n	neutrals
s	sonic passage
∞	far downstream asymptotic value
$\parallel$	parallel to the flow (streamwise).
$\perp$	transverse to the flow

*Graduate student
†Associate Professor
‡This work was sponsored by AFOSR Grant 86-0119

1 Introduction

This paper focuses on the role that an upstream flux of charged particles may have on the gas-plasma transition at the inlet of a magnetoplasmadynamic thruster. Steady-state "ignition" is defined here as the condition when this ionizing zone is fixed at the inlet wall, making the wall boundary condition a critical ignition factor.

This problem has been considered in other works as well, although the details of the ionizing zone are ignored. These models do yield significant results, but are not capable of looking into failure modes, i.e., non-ignition. Seals [8] very early on considered basic finite rate effects in a thruster and concluded that the most effective ionisation (and heating) occurs at subsonic speeds; however, the problem is formulated for an applied field device where low ionization fractions are tolerable for significant parts of the channel. Brushlinskii [1] modelled the ionizing zone as a discontinuous jump tripped whenever the temperature reaches a critical value. Kuriki [4] follows the plasma deflagration model of Cheng [2] in modelling the injection

Scale	Time Scale	Length Scale
Magnetic	$\tau_m = \frac{1}{\mu_o \sigma u_{ref}^2}$	$\Lambda_m = \frac{1}{\mu_o \sigma u_{ref}}$
Ambipolar	$(\tau_d)_\perp = \frac{h^2}{D_a}$	$(l_d)_\perp = \sqrt{\frac{D_a}{u_{ref}}}$
	$(\tau_d)_\parallel = \frac{D_a}{u_{ref}^2}$	$(l_d)_\parallel = \frac{D_a}{u_{ref}}$
Ionization	$\tau_i = \frac{n_e}{\dot{n}_e}$	$l_i = \tau_i u_{ref}$

Table 1: Various Scales in MPD Flows

region of an MPD thruster. The ionization zone is considered to be at the leading edge of a deflagration-like wave traveling against the flow. These two works yield reasonable jump conditions if one assumes that a transition occurs, but do not shed any light on the structure of the transition itself.

Two models will be considered: first a simple constant speed case, and then an accelerating case in which self-field fluid-magnetic field interactions are allowed. A quasi-one dimensional approach is taken, including both axial and transverse (with an assumed transverse distribution of density) ion slip, and collisional ionization. The flow will also be assumed to be isothermal, which simplifies the model. The constancy of T_e is justifiable on the basis of the combination of a large ionization energy sink plus strong electron heat conduction and zero electron heat flux at the walls (electron-repelling). The propellant will be argon.

While these models can not realistically reflect the 2 and 3 dimensional physics at the inlet of an MPD thruster, they do isolate the interaction between the convective, diffusion and collisional reaction processes. For reference, table 1 lists several of the time and length scales of relevance here. The goal is to determine which process or processes controls the transition, how thick the ionising front is, and what the steady flow ignition conditions are.

2 The Inlet Flow Model

In order to focus on the ignition process itself, the propellant is assumed to be injected through a porous backplate. This results in essentially a one dimensional (the streamwise direction) flow problem.

Before getting into the details, it is useful to consider the conditions expected in the ambient (downstream) plasma. Table 2 shows typical self-field MPD bulk properties. These values will be used as a reference. Some variables will be familiar, and the others will be defined below.

2.1 Equations of Motion

The steady state, quasi-one dimensional equations of motion for this configuration are overall and electron continuity, overall momentum, and a magnetic field equation, respectively, which can be written as:

Variable	Typical Value
T_e	$10000K - 30000K$
T_H	$1000K - 10000K$
$\dot{m}$	$0.005\frac{kg}{s}$
h	$0.02m$
L	$0.2m$
σ	$1000Si - 4000Si$
G	$7.5 \times 10^{24}\frac{m^{-2}}{s}$
C_e	$5 - 10 \times 10^{20} m^{-1} s^{-1}$
Λ_m	$0.05m$

Table 2: Typical values in MPD Flows

$$(n_e + n_n)u = G \tag{1}$$

$$\frac{dn_e u}{dx} = -\frac{dn_e V_i}{dx} - \frac{D_a n_e}{h^2} + \dot{n}_e \tag{2}$$

$$m_i(n_e + n_n)u^2 + p + \frac{B_z^2}{2\mu_o} = F \tag{3}$$

$$\frac{d}{dx}[\frac{5}{2}n_e k_B T_e] = \frac{d}{dx}[K_e \frac{dT_e}{dx}] + \vec{E}\cdot\vec{j} - E_i \dot{n}_e \tag{4}$$

$$\frac{dB}{dx} = -\mu_o j = -\mu_o \sigma[E - uB] \tag{5}$$

where n_e is the electron (and ion) number density and n_n is the neutral particle number density, u is the bulk speed, p is the pressure, B is the magnetic field, T_e is the electron temperature, E and j are the electric field and current density, and G and F are constants of the flow. $V_j = u_j - u$ is the species j slip speed. In equation 2, the transverse ambipolar diffusion, $\frac{D_a n_e}{h^2}$, is included (with an assumed parabolic distribution of n_e in the transverse direction so that h is actually $\frac{1}{\sqrt{12}}$ of the actual channel height) in order to allow a balance to be struck far downstream of the ionization layer.

2.2 Ionizing Collisions

The collisional ionization rate is assumed to be primarily due to electron-neutral collisions (local collisional recombination is ignored since we assume that the ionization fraction is always far below its equilibrium value). We use the rate coefficients for two-body continuum-ground state collisions derived in [9], (but neglecting the effects of the excited states):

$$\dot{n}_e = S_{ion} n_e n_n (m^{-3} s^{-1})$$

where the ionization coefficient is ([9]):

$$S_{ion} = 7.2787 * 10^{-12} * 0.295^{\Theta_{ion}} (m^3 s^{-1}) \quad (6)$$

$\Theta_{ion} = \frac{E_{ion}}{k_B T_e}$. For argon, $E_{ion} = 15.7eV$.

2.3 Conductivity

Even with the constant temperature assumption, the conductivity may vary as a function of the ionization fraction. This behavior is seen at low α, and may be expressed as [5]:

$$\sigma = \frac{A\alpha}{B(1-\alpha)T_e^{\frac{1}{2}} + D\alpha T_e^{-\frac{1}{2}}}$$

with $A = 2.81 \times 10^{-8}$, $B = 2.6 \times 10^{-16}$, $D = 3.62 \times 10^{-5}$. If the temperature is constant, then a reference conductivity can be calculated at the high α end: $\sigma_{ref} = \frac{A}{D} T_e^{\frac{3}{2}}$, and we can write

$$\frac{\sigma}{\sigma_{ref}} = \frac{\alpha}{\alpha + (1-\alpha)q} = \frac{1}{1 + (\frac{1}{\alpha} - 1)q} \quad (7)$$

$$q(T_e) = \frac{B}{D} T_e^2 = 7.2 \times 10^{-12} T_e^2$$

q is roughly the minimum ionization fraction for Coulomb collision dominance. $q \approx 0.001$ results from our choice of typical channel conditions. The reference conductivity would be approximately 1000 to 4000 Si.

2.4 Heat Conduction

Although the energy equation will be neglected in this work, we need to consider the validity of our isothermal assumption. Hence, the ambipolar diffusion and heat conduction scales will be compared to see if temperature variations may be left out for this first look at the inlet problem.

The thermal conductivity for the plasma is [7]:

$$K_e = \frac{1.7142 k_B^2 T_e \sigma}{e^2}$$

Comparison of the reaction-diffusion scale to that of heat conduction will reveal whether temperature can be assumed fixed in the ionizing region. The significant parameter here is a Lewis number:

$$Le = \frac{5}{2} \frac{k_B n_{ref} D_a}{K_e}$$

which becomes

$$L_e = \frac{1.46 C_a [B(1-\alpha)T_H^{\frac{1}{2}} + D\alpha T_e^{-\frac{1}{2}}]}{A k_B T_e}$$

so that $L_e = L_e(T_e, T_H, \alpha)$ (and the α dependence only appears at low α). (Note: the constants A, B and D are the same ones used in the previous subsection on conductivity.) For our "typical" MPD thruster conditions, $Le \approx O(10^{-2})$. Thus, the temperature may vary on a scale much longer than the diffusion-reaction scale, so that it is effectively frozen in the ionizing region. This assumption will be used for the rest of the paper.

3 Ion Slip

The streamwise slip of ions plays an important role in this work, so some care is taken in evaluating it. We present an alternative to Fick's Law. Starting with the 1-dimensional neutral momentum equation, in which electron-neutral collisional forces are neglected compared to ion-neutral forces,

$$m_i n_n v_n \frac{dv_n}{dx} = -\frac{dp_n}{dx} + m_i n_n n_e \bar{c}_{in} Q_{in} (V_i - V_n) \quad (8)$$

we assume that $|u_n - u| = V_n \ll u$ everywhere, so that

$$n_n v_n \frac{dv_n}{dx} \approx n_n u \frac{du}{dx}$$

Overall mass continuity requires that $n_n V_n + n_e V_i = 0$, and the neutral pressure is

$$p_n = k_B n_n T_H$$

With constant T_H, we can rewrite equation 8:

$$m_i n_n u \frac{du}{dx} = -k_B T_H \frac{dn_n}{dx} + m_i n_H n_e \bar{c}_{in} Q_{in} V_i \quad (9)$$

where $n_H = n_e + n_n$ is the number density of the heavy particles. Solving for $n_e V_i$, the ion slip flux,

$$n_e V_i = \frac{1}{n_H \bar{c}_{in} Q_{in}} \left(n_n u \frac{du}{dx} + \frac{k_B T_H}{m_i} \frac{dn_n}{dx} \right) \quad (10)$$

If we use the ambipolar diffusion coefficient [7]:

$$D_a = \frac{k_B (T_e + T_H)}{m_i \bar{c}_{in} Q_{in} n_H} (\frac{m^2}{s}) \quad (11)$$

as well as the definition of the Bohm velocity:

$$v_B = \sqrt{\frac{k_B (T_e + T_H)}{m_i}} \quad (12)$$

then equation 10 can be recast as:

$$n_e V_i = D_a \left(\frac{n_n u}{v_B^2} \frac{du}{dx} + \theta \frac{dn_n}{dx} \right) \quad (13)$$

$$\theta \equiv \frac{T_H}{T_e + T_H} \tag{14}$$

If we assume that the acceleration term is negligible and that there is no total pressure gradient ($\theta \frac{dn_n}{dx} = -\frac{dn_e}{dx}$), Fick's law results:

$$(n_e V_i)_F = -D_a \frac{dn_e}{dx} = D_a n_H \left(\frac{\alpha}{u}\frac{du}{dx} - \frac{d\alpha}{dx} \right) \tag{15}$$

However, retaining the inertia term and making no assumption about the total pressure gradient is more realistic, especially due to the large acceleration present in the inlet region. In this case, using the overall continuity equation (1), and the definition of the ionization fraction, $\alpha \equiv \frac{n_e}{n_H}$ in 13:

$$n_e V_i = D_a n_H \theta \left((1-\alpha)(\frac{u^2}{\theta v_B^2} - 1)\frac{1}{u}\frac{du}{dx} - \frac{d\alpha}{dx} \right) \tag{16}$$

Note that, for this alternative formulation, acceleration at $u < \sqrt{\theta} v_B$ yields backward ion diffusion (relative to the flow) - the neutrals are moving forward at a faster speed than the ions. In this regime, the slip is gradient dominated. Acceleration at $u > \sqrt{\theta} v_B$ means that the ions are moving faster than the neutrals. (Note that $\sqrt{\theta} v_B = \sqrt{\frac{p_H}{m_H n_H}}$ is roughly the heavy particle thermal speed.)

The ambipolar diffusion coefficient can also be expressed as

$$D_a = \frac{C_a}{n_H}$$

where $C_a = D_a n_H$ is a function of temperature only. Using the form for D_a in equation 11, C_a is

$$C_a = 1.274 * 10^{19} \left(1 + \frac{T_e}{T_H} \right) \sqrt{T_H} (m^{-1} s^{-1})$$

Note that while S_{ion} is a strong function of T_e, C_a is a fairly weak function of T_e and T_H. If the ion slip

4 Constant Speed Ignition

The simplest case considered is that of a constant speed. This is valid only if the pressure and magnetic field do not vary enough to accelerate the propellant significantly in the transition layer. This is essentially the first case analysed in section 2 of [10]. Only equation 2, the electron/ion continuity equation, remains.

It is assumed that the wall becomes slightly negatively charged due to initial random electron flux, so that it is electron repelling. This makes the boundary condition defining the wall:

$$(u n_e + n_e V_i)_o = -n_{eo} v_B \tag{17}$$

or, the ions reach the wall at $u_i = u + V_i = v_B$, the Bohm velocity.

We assume that all of the variables approach constant values asymptotically as x approaches ∞. While an actual MPD channel would not reach these local balance conditions, this is superior to a completely arbitrary condition and pins the solutions down to reasonable downstream plasma properties. This requires $\dot{n}_e = \frac{D_a n_e}{h^2}$ at ∞ (far downstream) in equation 2, or:

$$S_{ion}(n_n)_\infty = \frac{(D_a)_\infty}{h^2} \tag{18}$$

For this case, Fick's Law is used (note that for constant speed, the two ion slip methods differ only by the factor θ). Keeping in mind that constant speed means constant overall density, we then define the ambipolar flux, $\Gamma = -n_e V_i$ as

$$\Gamma = D_a \frac{dn_e}{dx} = D_a n_H \frac{d\alpha}{dx} \tag{19}$$

Equation 2 then becomes

$$\frac{u\Gamma}{D_a} = \frac{d\Gamma}{dx} - \frac{D_a n_e}{h^2} + \dot{n}_e \tag{20}$$

and dividing 20 by equation 19, which amounts to changing to α as the independent variable, and nondimensionalising, with $\gamma = \frac{\Gamma}{G}$:

$$\frac{d\gamma}{d\alpha} = 1 - \delta_1^2 \frac{\alpha(\alpha_\infty - \alpha)}{\gamma} \tag{21}$$

where, as implied by equation 18, $1 - \alpha_\infty = \frac{D_a}{S_{ion} n_H h^2}$, and we have introduced the parameter

$$\delta_1 = \frac{\sqrt{D_a n_H^3 S_{ion}}}{G} = \frac{\sqrt{C_a S_{ion}}}{u} \tag{22}$$

Alternatively, we can eliminate the temperature-sensitive $S_{ion}(T_e)$ by use of the end condition, giving

$$\delta_1 = \frac{C_a}{Gh\sqrt{1-\alpha_\infty}} \tag{23}$$

Successful trajectories must travel from the wall condition to the downstream balance ($\gamma = 0$, $\alpha = \alpha_\infty$) singularity. The physically valid range of δ_1 can be obtained by examining the behavior near the singularity at $\alpha = \gamma = 0$, where the slope is [10]:

$$\left(\frac{d\gamma}{d\alpha} \right)_* = \frac{1}{2} \pm \sqrt{\frac{1}{4} - \delta_1^2 \alpha_\infty}$$

If δ_1 is smaller than $\frac{1}{\sqrt{4\alpha_\infty}}$, there will be two real slopes, and the trajectories approach the $\alpha = \gamma = 0$ point along the smaller of them. The slope from the wall condition, equation 17 is now

$$\left(\frac{d\gamma}{d\alpha}\right)_o = \frac{v_B}{u_o} + 1 \qquad (24)$$

These two meet only at the origin itself, where the ion density approaches zero exponentially on the upstream side, and an infinite ionization length is implied. Physically, the ionizing region is blown out of the channel.

When $\delta_1 > \frac{1}{\sqrt{4\alpha_\infty}}$, the singularity becomes a spiral point and the trajectory arriving from the downstream singularity crosses the wall condition (eq. 24) at finite α and γ, which corresponds to a finite ionization layer thickness (from $dx = \frac{C_a}{G\gamma} d\alpha$).

From the forms (22, 23) given for δ_1 this condition for "ignition in a finite distance" is then either

$$u < 2\sqrt{\alpha_\infty C_a S_{ion}(T_e)} \qquad (25)$$

or

$$Gh < 2\sqrt{\frac{\alpha_\infty}{1-\alpha_\infty}} C_a \qquad (26)$$

Of these, 25 is the more direct expression, since it makes no use of the assumption of a downstream ionization-diffusion balance. By the same token, it leaves the sensitive ionization rate function S_{ion} unspecified, and then indicates that the flow velocity in the ionization region (presumably before significant magnetic acceleration) should be below a temperature-dependent limit. Using argon parameters, this limitation is displayed along with the "ionization thickness" in figure 1, from [10]. At $T_e \approx 1eV$ $(11600K)$ the "blow-out" velocity is about $300\frac{m}{s}$, and the thickness is a few mm.

If the asymptotic limit is accepted, the relevant form of the ignition criterion is equation 26, where T_e does not appear in a sensitive manner. Recalling the definitions of G and h, this can be recast as

$$\frac{\dot{m}}{w} < m_i C_a \sqrt{48\frac{\alpha_\infty}{1-\alpha_\infty}} \qquad (27)$$

where w is the depth (along $\vec{B}$). For typical values of $\frac{\dot{m}}{w}$ and of m_i and $C_a = D_a n_H$, satisfaction of equation 27 requires α_∞ to be fairly close to unity.

5 Ignition in Accelerating Flows

We now drop the assumption of constant speed. This allows us to analyze the interaction between the behavior of the magnetic field and the ionization process. In [10], this was done by assuming a local balance for the electron energy equation. Here the local balance assumption is dropped in favor of a constant temperature. Acceleration may be due to two sources: magnetic or thermal (pressure gradients; for the constant temperature assumption, this corresponds to density gradients).

5.1 Formulation

We start with the differential form of the momentum equation (3):

$$m_i(n_e + n_n)u\frac{du}{dx} + \frac{d}{dx}\left(p + \frac{B_z^2}{2\mu_o}\right) = 0 \qquad (28)$$

The pressure for a two temperature, electrically neutral plasma is

$$p = n_e k_B(T_e + T_H) + n_n k_B T_H$$

Using the definitions of the Bohm velocity and θ,

$$p = m_i n_H v_B^2(\alpha + (1-\alpha)\theta) \qquad (29)$$

Here, because of the acceleration, the alternative version for the ion is used, so that, using equation 16, we define the flux, $\Gamma = -n_e V_i$, as

$$\Gamma = -D_a n_H \theta\left((1-\alpha)(\frac{u^2}{\theta v_B^2} - 1)\frac{1}{u}\frac{du}{dx} - \frac{d\alpha}{dx}\right) \qquad (30)$$

which may be rewritten as:

$$\frac{d\alpha}{dx} = \frac{\Gamma}{C_a\theta} + (1-\alpha)(\frac{u^2}{\theta v_B^2} - 1)\frac{1}{u}\frac{du}{dx} \qquad (31)$$

This equation , along with the following three, constitute the equations of motion for the quasi-one-dimensional isothermal flow problem:

$$\frac{du}{dx} = \frac{-\frac{v_B^2(1-\vartheta)\Gamma}{C_a u} + \frac{\vartheta B}{m_i G}\sigma(E - uB)}{1 - \alpha(1-\theta) - \frac{\theta v_B^2}{u^2}} \qquad (32)$$

$$\frac{d\Gamma}{dx} = G\frac{d\alpha}{dx} + \frac{C_a\alpha}{h^2} - S_{ion} n_H^2 \alpha(1-\alpha) \qquad (33)$$

$$\frac{dB}{dx} = -\mu_o\sigma(E - uB) \qquad (34)$$

Nondimensionalizing these equations will allow us to analyse them parametrically. Defining reference values $u_{ref} = \frac{B_*^2}{2\mu_o m_i G}$, and $l_{ref} = \Lambda_m = \frac{1}{\mu_o\sigma u_{ref}}$, then the new variables are $\bar{u} = \frac{u}{u_{ref}}$, $\gamma = \frac{\Gamma}{G}$, $b = \frac{B}{B_*}$, and $\xi = \frac{x}{\Lambda_m}$. The resulting nondimensional equations of motion are:

$$\frac{d\bar{u}}{d\xi} = \frac{-\frac{\beta(1-\vartheta)\gamma}{\epsilon p^2} + \frac{2\vartheta b}{f}}{1 - \alpha(1-\theta) - \frac{\theta\beta}{\bar{u}^2}} \qquad (35)$$

$$\frac{d\alpha}{d\xi} = \frac{\gamma}{\epsilon_D \theta} + (1-\alpha)\left(\frac{\bar{u}^2}{\theta\beta} - 1\right)\frac{1}{\bar{u}}\frac{d\bar{u}}{d\xi} \tag{36}$$

$$\frac{d\gamma}{d\xi} = \frac{d\alpha}{d\xi} + \epsilon_w \alpha - \frac{\lambda\alpha(1-\alpha)}{\bar{u}^2} \tag{37}$$

$$\frac{db}{d\xi} = -\frac{\bar{E} - \bar{u}b}{1 + (\frac{1}{\alpha} - 1)q} \tag{38}$$

where for convenience we define

$$f = \frac{1 + (\frac{1}{\alpha} - 1)q}{\bar{E} - \bar{u}b} = -\left(\frac{db}{d\xi}\right)^{-1}$$

The parameters in addition to those used previously are:

$$\lambda = \frac{\Lambda_m G S_{ion}}{u_{ref}^2} = \frac{\Lambda_m}{l_{ion}}$$

$$\beta = \frac{v_B^2}{u_{ref}^2}$$

$$\epsilon_D = \frac{(C_e)\mu_o \sigma_{ref} u_{ref}}{G} \approx \frac{(l_d)_\parallel}{\Lambda_m}$$

$$\epsilon_w = \frac{C_e \Lambda_m}{G h^2}$$

θ (eq. 14) should be small near the inlet, and we use $\theta = 0.1$ here. The parameters λ, ϵ_D and ϵ_w are sensitive to electron temperature, particluarly at low T_e. Figure 2 shows $\lambda(T_e)$. Figure 3 shows both ϵ_D and q and figure 4 shows ϵ_w. β is a measure of the gas pressure divided by the magnetic pressure, and the value of β is roughly 0.05 for the conditions considered.

The first downstream boundary condition will be that $\bar{E} = \bar{u}b$, which implies an infinite magnetic Reynolds number, or $\xi \to \infty$. This motivates us to choose the magnetic field itself as the independent variable. Dividing the three other equations of motion (35, 36, 37) by equation 38, we arrive at the following set of equations:

$$\frac{d\bar{u}}{db} = \frac{f\beta(1-\theta)\frac{\gamma}{\epsilon_D q} - 2\theta b}{1 - \alpha(1-\theta) - \frac{\theta\beta}{q^2}} \tag{39}$$

$$\frac{d\alpha}{db} = -f\frac{\gamma}{\epsilon_D \theta} + (1-\alpha)\left(\frac{\bar{u}^2}{\theta\beta} - 1\right)\frac{1}{\bar{u}}\frac{d\bar{u}}{db} \tag{40}$$

$$\frac{d\gamma}{db} = \frac{d\alpha}{db} - f\left(\epsilon_w \alpha - \frac{\lambda\alpha(1-\alpha)}{\bar{u}^2}\right) \tag{41}$$

The second downstream (∞) boundary condition is the same balance between transverse ambipolar diffusion and ionization used in the constant speed case. Refering back to equation 18, this is:

$$1 - \alpha_\infty = \frac{C_e u_\infty^2}{S_{ion} G^2 h^2} = \frac{\epsilon_w \bar{u}_\infty^2}{\lambda} \tag{42}$$

Additional boundary conditions are the conditions at the injector wall, and the internal boundary conditions at the sonic passage point. The injector wall condition (17) is now

$$-\gamma_o + \alpha_o(1 + \frac{\sqrt{\beta}}{\bar{u}_o}) = 0$$

Since the speeds and ionization fraction are positive, $\gamma_o > 0$, which we expect, as the ions diffuse backwards towards the recombination sink at the inlet wall.

If subsonic injection is assumed, then smooth passage through a "sonic point" [6] is required in the steady state. The sonic point is characterized as a singularity that occurs when the denominator of the $\frac{d\alpha}{db}$ equation is identically zero at some $b = b_s$. In order to be physically possible, the numerator must be zero at the same b_s. This means that

$$\bar{u}_s^2 = \frac{\theta\beta}{1 - \alpha_s(1-\theta)} \tag{43}$$

$$\gamma_s = \frac{2\theta\epsilon_D \bar{u}_s b_s}{\beta(1-\theta) f_s} \tag{44}$$

Here we see that $\gamma_s > 0$. Thus the slip is still important at the sonic passage point, and the ions are still moving slower than the neutrals there.

The equations of motion (39, 40, 41) were solved numerically, starting at the downstream singularity, $\bar{E} = \bar{u}b$ and integrating to the wall at $b = 1$. The marching scheme starts with an initial step using slopes calculated from the equations of motion linearised about $(\bar{u}, \alpha, \gamma) = (\bar{u}_\infty, \alpha_\infty, 0)$. To avoid the sonic passage singularity, another integration is carried out starting out at the sonic passage (b_s), using L'Hopital's rule to calculate $(\frac{d\alpha}{db})_s$. This second integration leg is then patched onto the downstream leg for a smooth solution. A 4^{th} order Runga-Kutta routine with variable steps was used throughout.

The solution scheme can be summarized as follows:

1. Select T_e, T_H, h; calculate the parameters λ, ϵ_w, ϵ_D, and β. T_e will have to be substantiated by a global energy balance to close the loop.

2. Select $\bar{E}$. This is, within limits, a free parameter, the value of which specifies a particular inlet/throat area ratio (as in [6]).

3. Guess (b_s, α_s) and integrate upstream from the sonic point, varying b_s until condition 17 is met. Integrate also downstream from the sonic point until divergence occurs (this is because of the spurious exponentially growing behavior associated with diffusion).

4. Guess b_∞, calculate the other downstream properties, including starting slopes, and integrate back towards the sonic point.

5. Adjust the b_* and b_∞ guesses until a smooth match is achieved.

5.2 Results and Discussion

Figures 5 to 8 show calculated results for a case with $T_e = 17500K = 1.51eV$, $T_H = 1950K$ ($\theta = 0.1$) and $\bar{E} = 0.4$, which corresponds to a small contraction ratio from inlet to throat. As discussed, calculations are carried out with b as an independent variable. The degree of ionization vs $b = \frac{B}{B_*}$ is shown in figure 5. The sonic point is indicated by a small circle. The somewhat imperfect blending of the upstream and downstream trajectories is noticeable slightly downstream of this sonic point. The calculated degree of ionization at the inlet wall is 5.396×10^{-4}, and it rises rapidly to 0.1876 at the sonic point, and 0.7 far downstream.

After the distance $\xi = \frac{x}{\Lambda_m}$ is calculated vs b, other variables can be shown vs ξ, as in figures 6, 7 and 8. Figures 6 and 7 show that, as expected, u and B evolve in a thickness $x \sim \Lambda_m$ ($\xi \sim 1$) to their final values. Figure 8 (on an expanded ξ scale) contains the important results about the ion slip. As required by the wall condition, $\gamma_o > 0$, namely, the ions slip backwards towards the inlet. This condition persists throughout the subsonic part of the flow, but reverses itself soon past the sonic point. In the supersonic region, the ions move faster than the neutrals, and the slip is forward ($\gamma < 0$). This situation is physically understandable: the backwards ion diffusion required to initiate conduction, and hence ionization, near the inlet wall is driven by the steep initial ionization gradient (despite the opposing density gradient), but the maximum diffusion velocity must be of the order of the speed of sound, and hence the existence of a subsonic layer is essential for ignition. This confirms qualitatively the results of the simple constant velocity analysis. On the other hand, figure 5 shows that the ionization continues throughout the acceleration layer, so that it is not strictly possible to separate a constant-velocity ionizing region.

These results are only indicative, however. The energy balance required to substantiate T_e has not yet been carried out (although $T_e \approx 1.5eV$ is close to observed values). Also, a parametric study is needed to identify ignition limits as a function of field $\bar{E}$. Smaller values of $\bar{E}$ correspond to larger inlet/throat area ratios, in which case ignition difficulties can be expected.

References

[1] Brushlinskii, K. V., Zaborov, A. M., etal, "Numerical modeling of plasma flow in high-current quasistationary plasma accelerators", Sov. J. Plasma Phys., Vol. 16, No. 2, pp. 79-85, Feb. 1990

[2] Cheng, D. Y., "Plasma Deflagration and the Properties of a Coaxial Plasma Deflagration Gun", Nuclear Fusion, Vol. 10, pp. 305-317, 1970

[3] Kilfoyle, D. B., Martinez-Sanchez, M., etal., "Spectroscopic Investigation of the Exit Plane of an MPD Thruster", IEPC-88-027, 1988

[4] Kuriki, K. and Suzuki, H., "Quasisteady MPD Arcjet with Anode Gas Injection", in *Electric Propulsion and its Applications to Space Missions*, Finke, R. C., editor, AIAA, Washington D.C., 1981

[5] Liberman, M. A. and Velikovich, *Physics of Shock Waves in Gases and Plasmas*, Springer-Verlag, New York, 1986

[6] Martinez-Sanchez, M., "The Structure of Self-Field Accelerated Plasma Flows", *Journal of Propulsion and Power*, Vol. 7, No. 1, Jan-Feb 1991

[7] Mitchener, M. and Kruger, C.H. Jr., *Partially Ionized Gases*, John Wiley and Sons, New York, 1973

[8] Seals, R. K. and Hassan, H. A., "Analysis of MPD Arcs with Nonequilibrium Ionization", *AIAA Journal*, Vol. 6, No. 12, December 1968

[9] Sheppard, E. J. and Martinez-Sanchez, M., "Nonequilibrium Ionization in MPD Thrusters", AIAA 90-2608, presented at the 21st IEPC, July 1990

[10] Sheppard, E. J., Chanty, J. M., and Martinez - Sanchez, M., "Local Analyses in MPD Thrusters: Diffusion - Reaction and Magnetodynamic Regimes", AIAA 91-2589, presented at the 27th JPC, June 1991

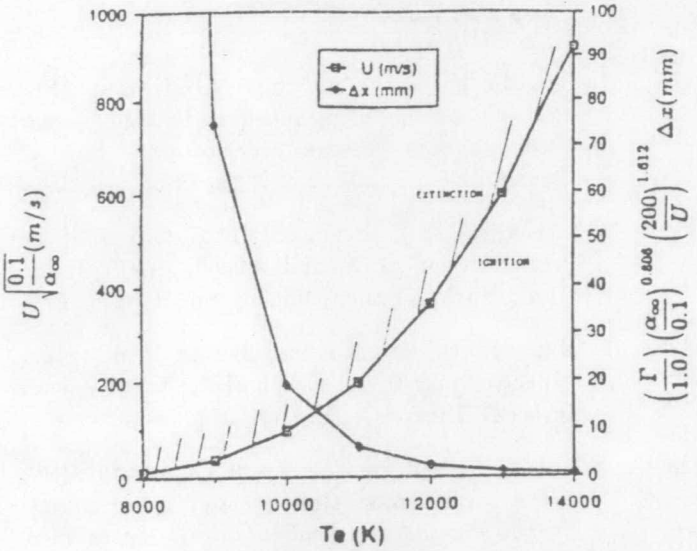

Figure 1: Ionizing layer thickness and maximum speed for steady ignition vs electron temperature from reference 10

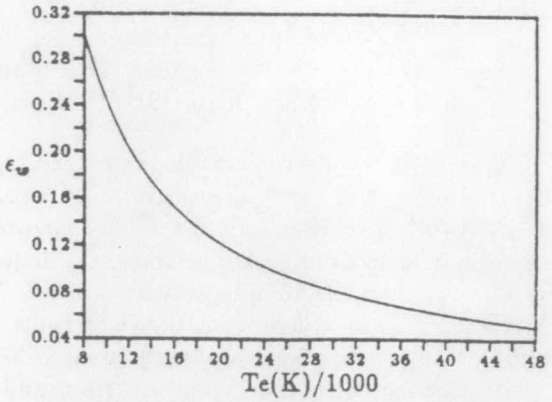

Figure 4: Parameter ϵ_ω vs T_e, $\theta = 0.1$

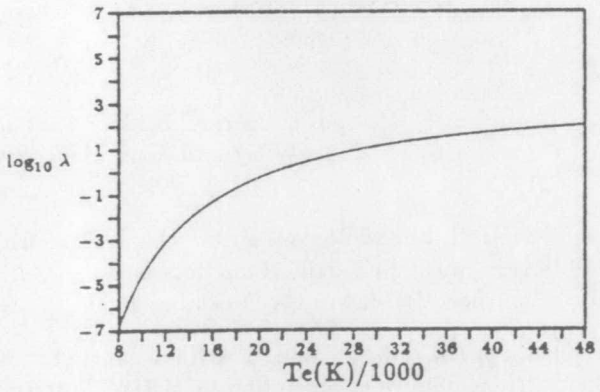

Figure 2: $\log_{10} of parameter \lambda$ vs T_e, $\theta = 0.1$

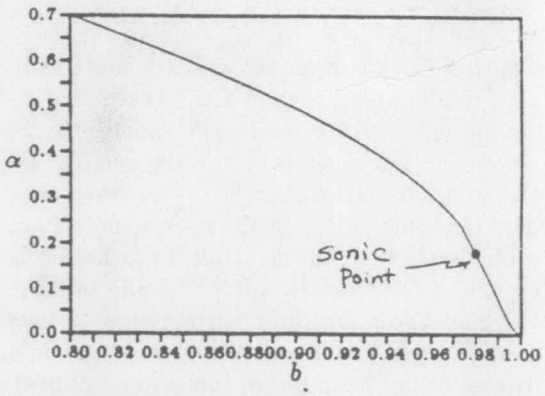

Figure 5: Ionization fraction α vs b

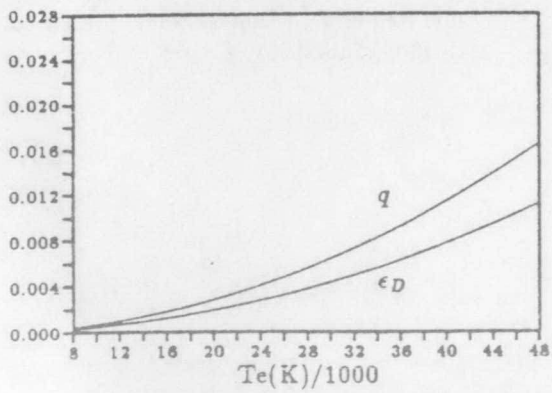

Figure 3: Parameters ϵ_D and q vs T_e, $\theta = 0.1$

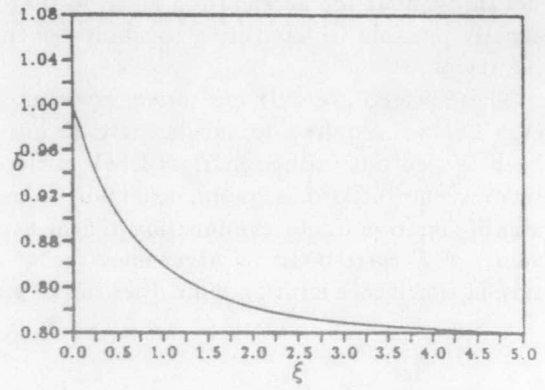

Figure 6: Magnetic field b vs ξ

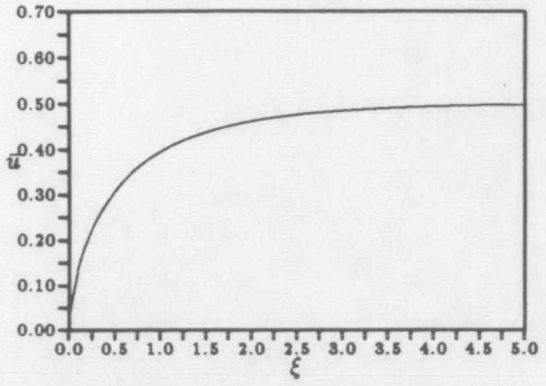

Figure 7: Plasma speed $\bar{u}$ vs ξ

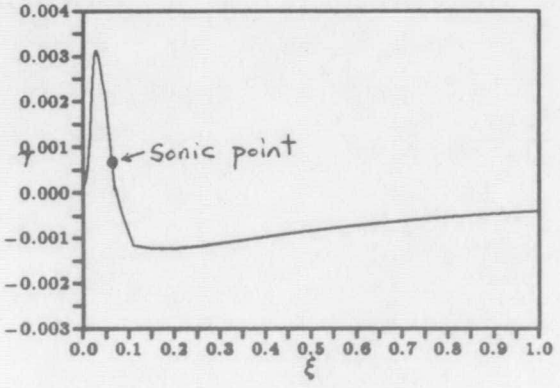

Figure 8: Ion slip γ vs ξ (note the expanded scale)